Supplementary Information

Combined effects of electrode morphology and electrolyte composition on single H_2 gas bubble detachment during hydrogen evolution reaction

Sunghak Park[a,b,c,*], Aleksandr Bashkatov[d,*], Jordy J. J. Eggebeen[c], Siyoung Lee[a], Detlef Lohse[e,f], Dominik Krug[d,e,*], and Marc T.M. Koper[c,*]

[a] Department of Future Energy Engineering, Sungkyunkwan University (SKKU), Suwon 16419, Republic of Korea

[b] SKKU Institute of Energy Science and Technology (SIEST), Sungkyunkwan University, Suwon 16419, Republic of Korea

[c] Leiden Institute of Chemistry, Leiden University, Leiden, the Netherlands

[d] Chair of Fluid Mechanics and Institute of Aerodynamics, RWTH Aachen University, Wüllnerstr. 5a, 52062 Aachen, Germany.

[e] Physics of Fluids Group, Max Planck Center Twente for Complex Fluid Dynamics, Faculty of Science and Technology, University of Twente, Enschede, the Netherlands

[f] Max Planck Institute for Dynamics and Self-Organization, Göttingen, Germany

E-mail: sunghak@skku.edu, a.bashkatov@aia.rwth-aachen.de, d.krug@aia.rwth-aachen.de, m.koper@lic.leidenuniv.nl

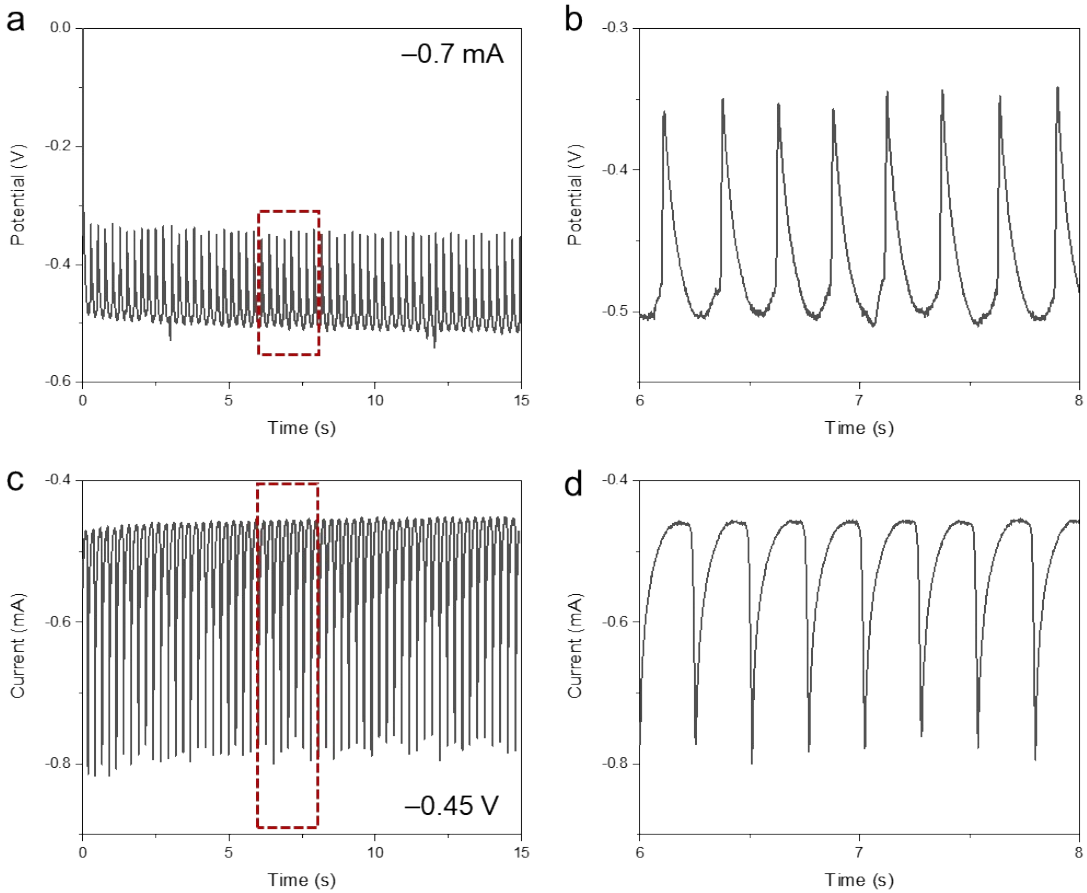

Supplementary Figure S1. *Electrochemical oscillations observed during chronopotentiometry (a, b) and chronoamperometry (c, d) using a polished Pt microelectrode after electrochemical pretreatment in 0.5 M H_2SO_4. In chronopotentiometry, a constant current of −0.7 mA was applied, while in chronoamperometry, the applied potential was −0.45 V_{RHE}. Supplementary Figure S1b and S1d show magnified vies of the red-dotted regions in Supplementary Figure S1a and S1c, respectively.*

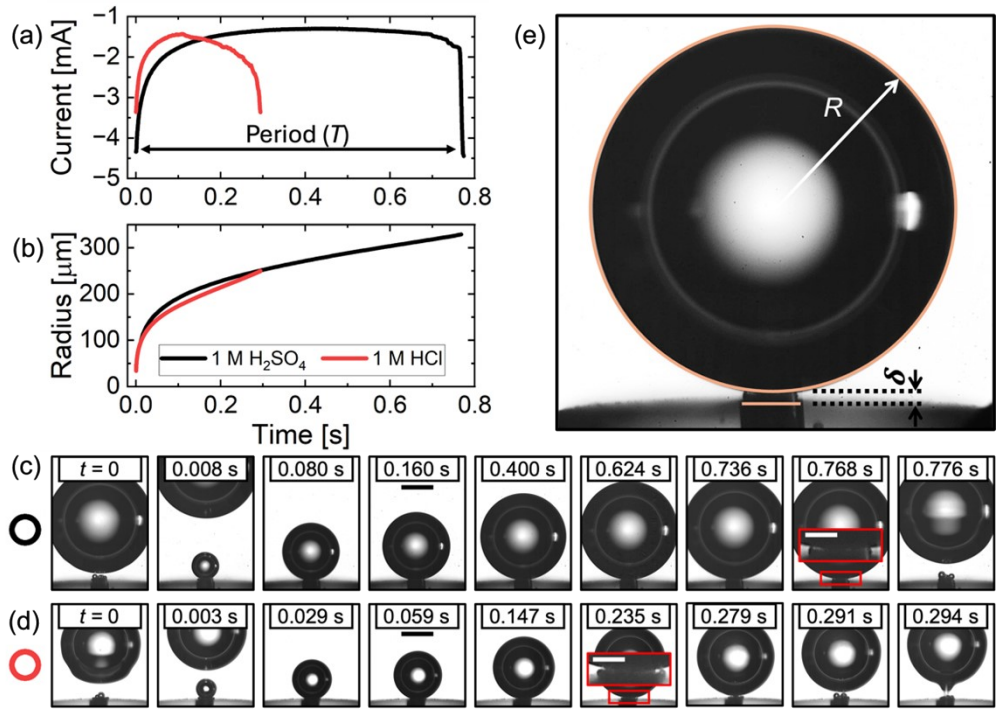

Supplementary Figure S2. *(**a-b**) The electric current and radius of the bubble throughout its evolution in 1 M H_2SO_4 (black curves) and 1 M HCl (red curves), supplemented with the corresponding snapshots in (**c**) 1 M H_2SO_4 and (**d**) in 1 M HCl. T is the period of the bubble evolution. The red insets in (**c-d**) zooms into the bubble's bottom region, highlighting the microbubble carpet sandwiched between the primary bubble and the electrode surface. Black scale bar represents 200 μm, and white scale bar within the inset is 50 μm. (**e**) An example of measuring the thickness of microbubbles' carpet, δ,. The experiments performed using a rougher surface at −1.3 V_{RHE} in 1 M H_2SO_4.*

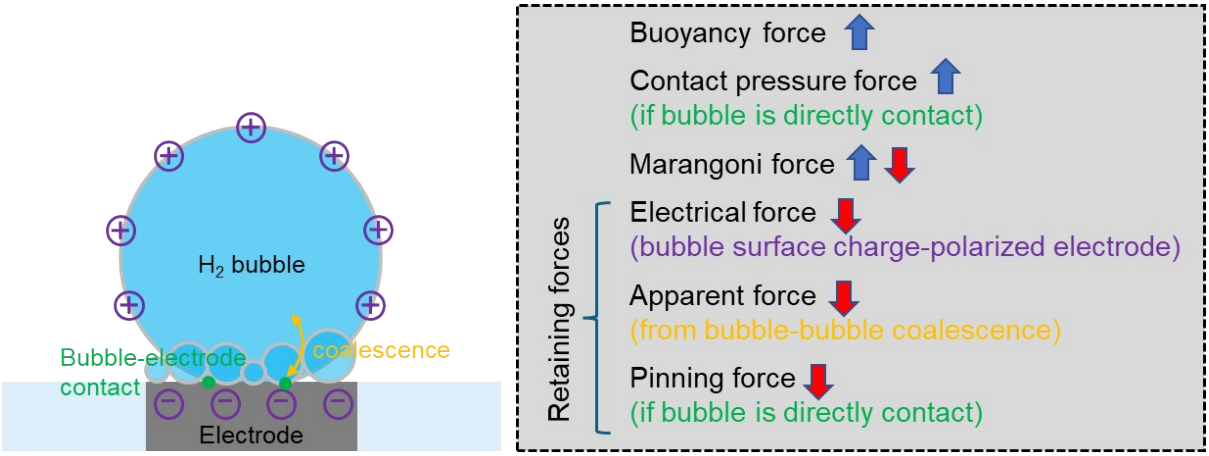

Supplementary Figure S3. *Schematic illustration of the possible forces acting on an H_2 gas bubble during the hydrogen evolution reaction in acid electrolytes. Note that bubble surface is positively charged in acid electrolytes, while the Pt electrode is negatively polarized during the hydrogen evolution reaction.*

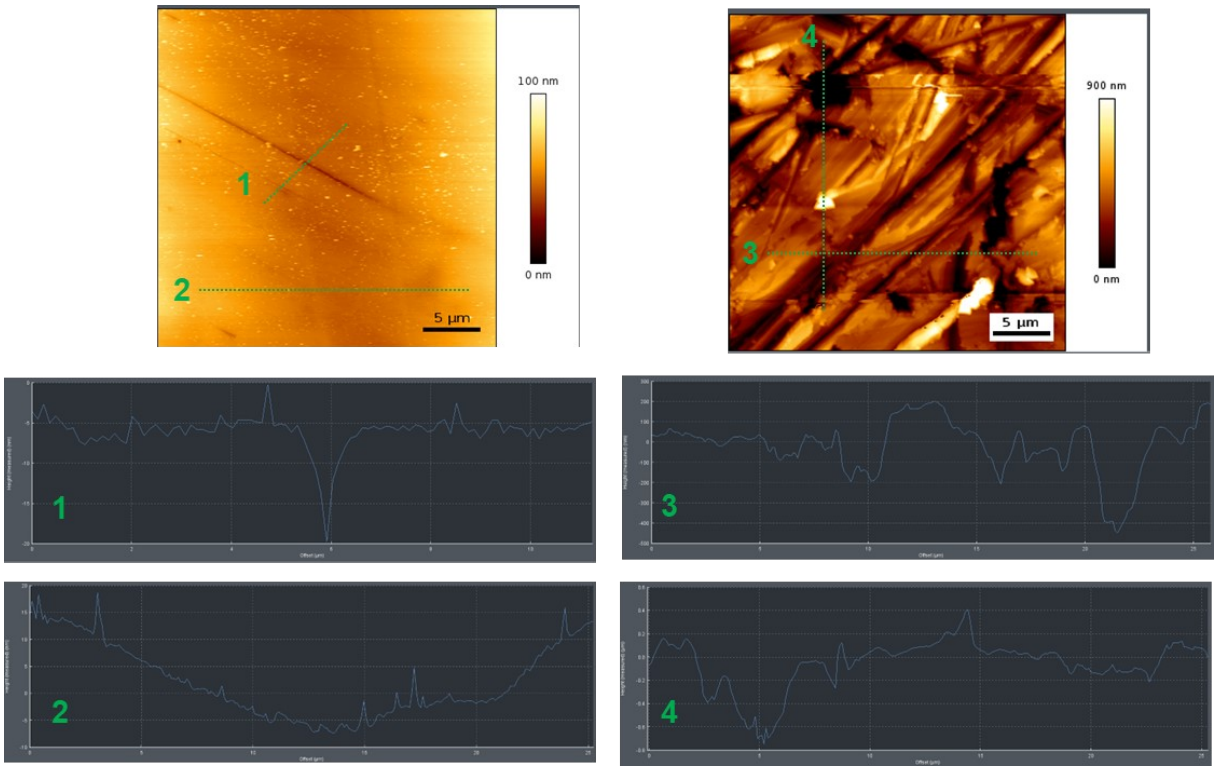

Supplementary Figure S4. *AFM height images and line profiles of Pt microelectrode surfaces with smoother (left) and rougher (right) morphologies. Line profiles were extracted from the lines indicated in AFM height images. Note that scale differs between the smoother and rougher surfaces.*

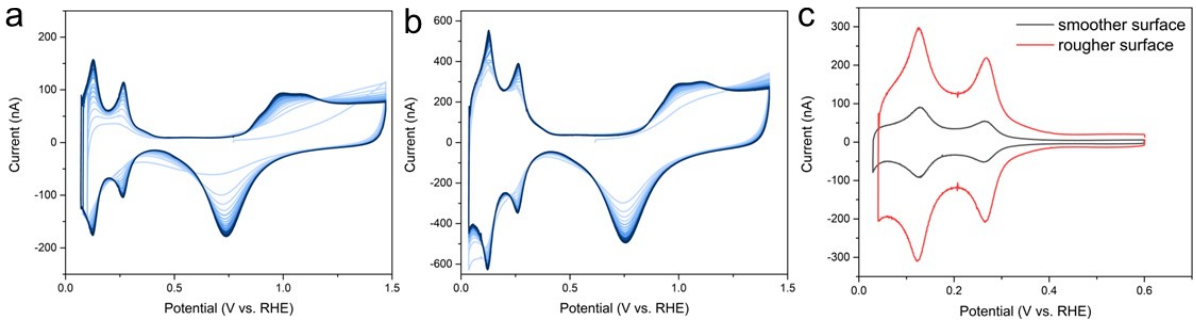

Supplementary Figure S5. *Blank voltammetry of Pt microelectrodes in 1 M H_2SO_4. (**a**) Cyclic voltammograms of the smoother surface during electrochemical pretreatment at a scan rate of 1 V s^{-1}. (**b**) Cyclic voltammograms of the rougher surface under the same pretreatment conditions. (**c**) Cyclic voltammograms highlighting the hydrogen adsorption/desorption peaks at a scan rate of 0.5 V s^{-1} after pretreatment.*

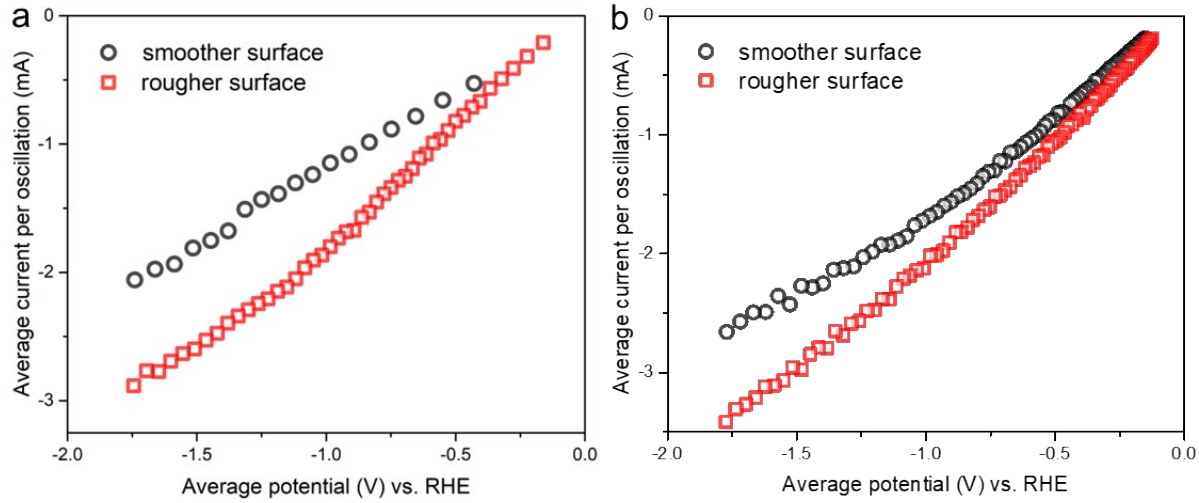

Supplementary Figure S6. *Average current per oscillation from Pt microelectrode #1 in 1 M H_2SO_4 (**a**) and 1 M HCl (**b**). Each average current is obtained from the oscillation in Figure 5a and 5d, respectively.*

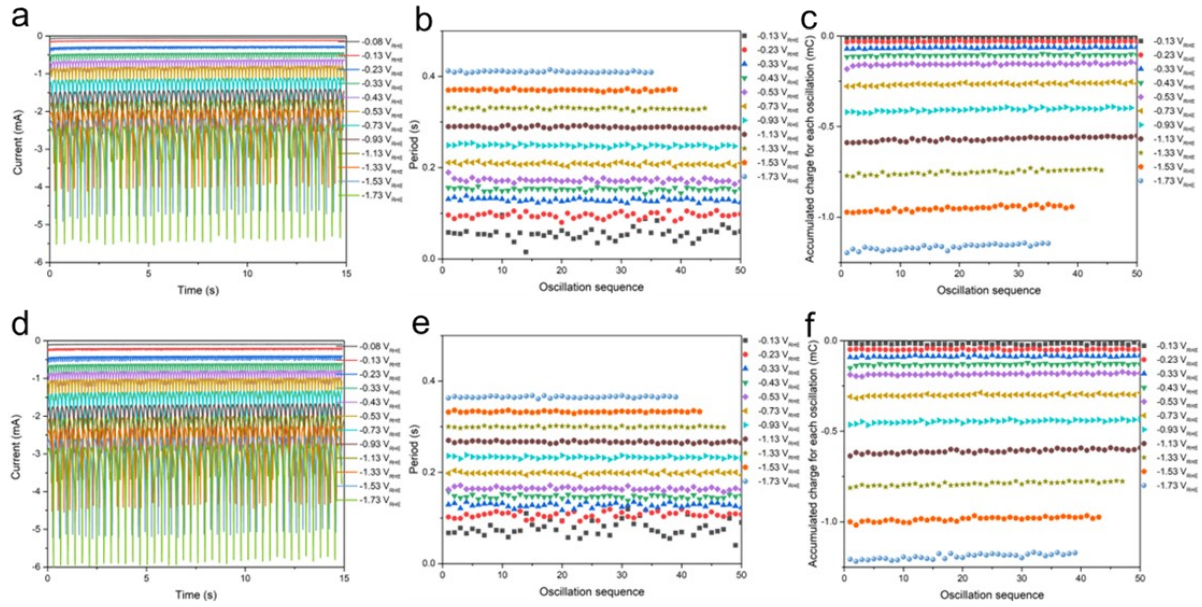

Supplementary Figure S7. *Electrochemical oscillation analysis through chronoamperometry in 1 M HCl. (**a-c**) Chronoamperometry (**a**), period (**b**), and accumulated charge per oscillation cycle (**c**) for the smoother surface of Pt microelectrode #3. (**d-f**) Chronoamperometry (**d**), period (**e**), and accumulated charge per oscillation cycle (**f**) for the rougher surface of Pt microelectrode #3.*

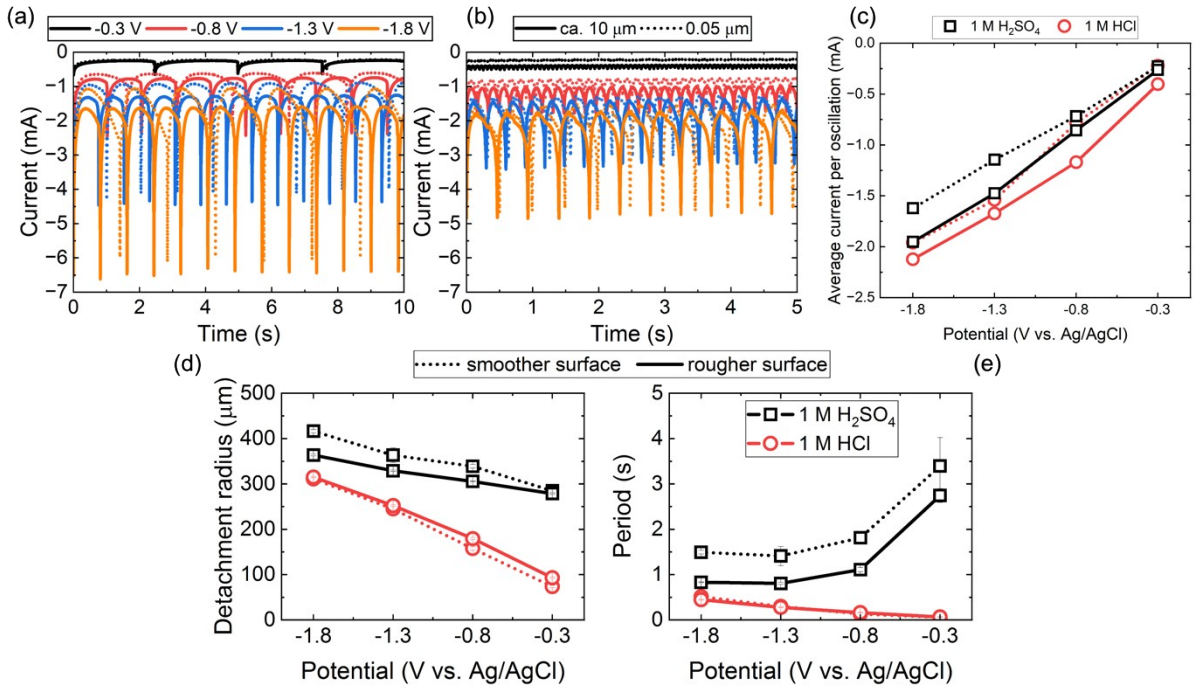

Supplementary Figure S8. *Electric current over time at constant potential in (**a**) 1 M H_2SO_4 and (**b**) 1M HCl. (**c**) The average current per oscillation, (**d**) detachment radius and (**e**) period as a function of applied potential. The dotted curves are for smoother electrode and solid curves are for rougher electrode.*

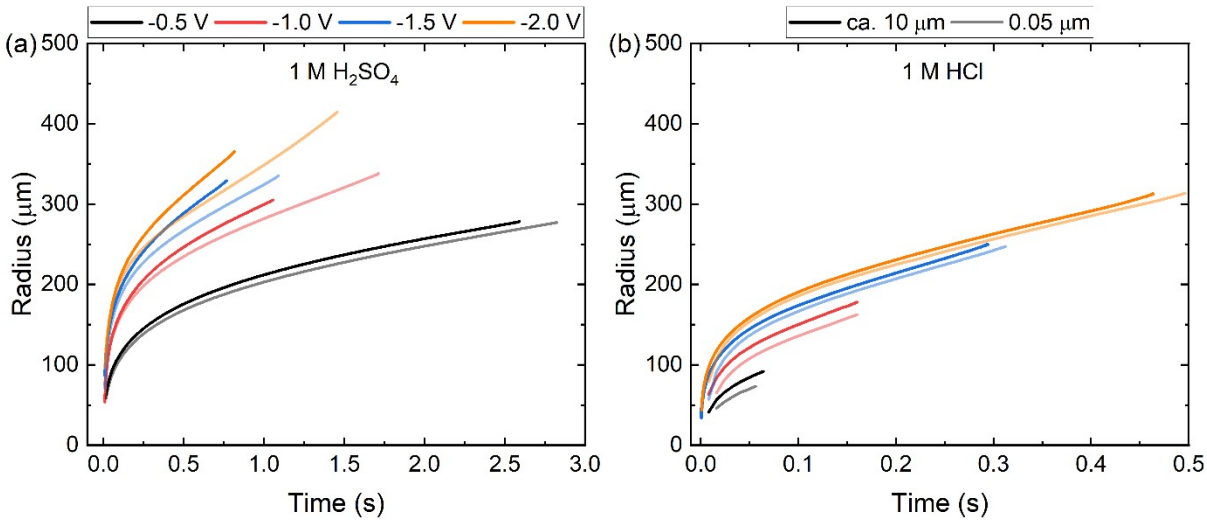

Supplementary Figure S9. *Radius of the bubble throughout its evolution at various potentials (vs. Ag/AgCl) and for different surface roughness in (**a**) 1 M H_2SO_4 and (**b**) 1 M HCl. Lighter curves mark the smoother surfaces, while darker curves correspond to the rougher surfaces.*

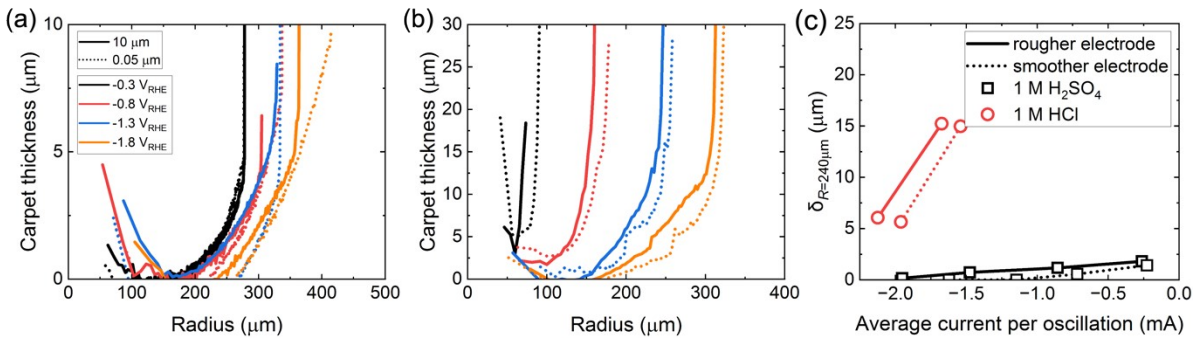

Supplementary Figure S10. *Thickness of the carpet as a function of the bubble radius throughout its evolution at various potentials (vs. Ag/AgCl) and for different surface roughness in (**a**) 1 M H_2SO_4 and (**b**) 1 M HCl. (**c**) Thickness of the carpet at a fixed bubble radius R = 240 μm as a function of average current per oscillation. The dotted curves are for the smoother electrode and solid curves are for the rougher electrode.*

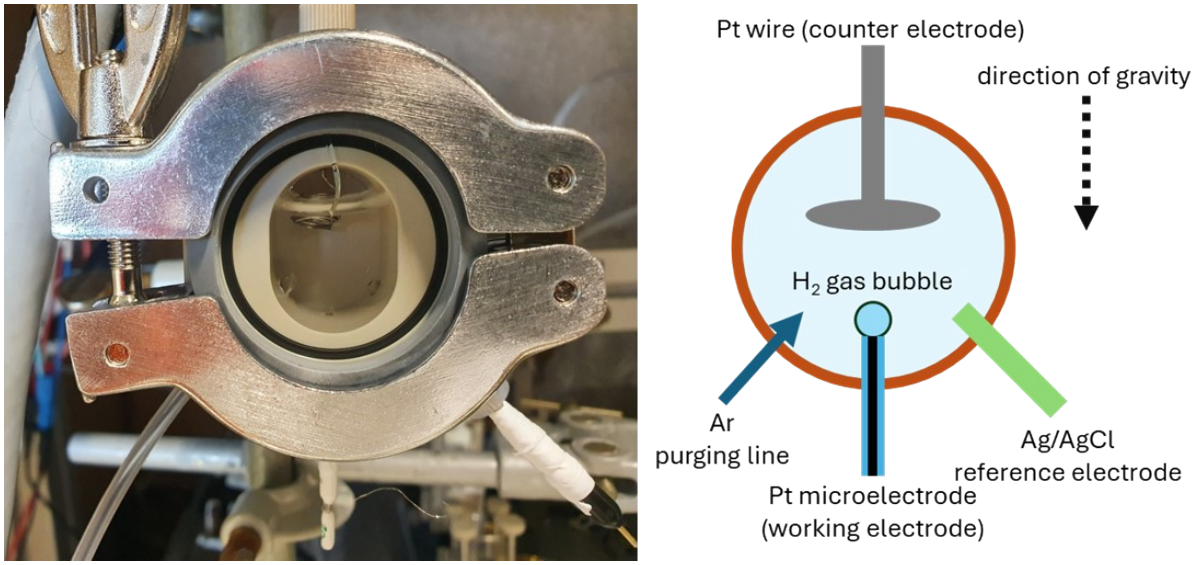

Supplementary Figure S11. *Photograph (left) and schematic illustration (right) of the experimental setup using a homemade electrochemical cell. The Pt microelectrode is oriented anti-parallel to the direction of gravity, allowing gas bubbles to detach freely due to buoyancy.*

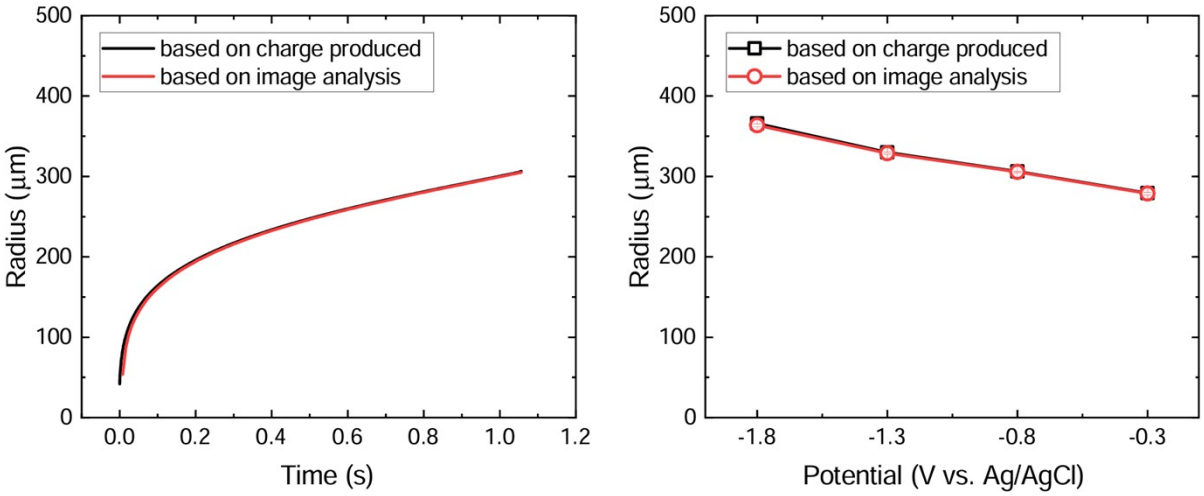

Supplementary Figure S12. *The evolution of bubble radius over time on a rougher surface at -0.8 V (vs .RHE) in 1 M H_2SO_4 (left). The averaged detachment radius at different potentials in 1 M H_2SO_4, determined from the analysis of 20 bubble evolution events (right). Error bars in the right figure demonstrate the standard deviation. The black lines document the radius calculated from electrochemical oscillation data using the formula described in experimental section, whereas the red lines represent the radius obtained from image analysis. The close agreement between the two methods validates the radius estimation based on electrochemical oscillation analysis.*